IPBI TN-2006-4
31 October 2006

Performance of Extraction Line Energy Spectrometers and Polarimeters at 1 TeV Center-of-Mass Collision Energy

Ken Moffeit, Takashi Maruyama, Yuri Nosochkov, Andrei Seryi and Mike Woods
SLAC

William P. Oliver
Tufts University

Eric Torrence
University of Oregon

Abstract

A study of beam distributions for 1 TeV center-of-mass collision energy at the ILC is presented for the 2 mrad and 14 mrad extraction lines. Beam losses between the IR and the Compton detector plane are given, and the backgrounds from the lost beam particles at the Compton Polarimeter Cherenkov detector are estimated. Beam energy losses due to synchrotron radiation in the magnets between the e^+e^- IR and the measurement of the energy are studied. Changes in the synchrotron radiation losses due to trajectory variations caused by beam collisions conditions at the e^+e^- IR are studied. The impact of these variations on the precision measurement of the energy is given. Variation in spin diffusion in the extraction lines due to beam collision conditions at the e^+e^- IR is studied, and its estimate on the uncertainty of the precision measurements of polarization is presented. Backgrounds from synchrotron radiation at the location of the energy spectrometer and polarimeter detectors are shown.

1. Introduction

Two Interaction Regions (IR) are being considered for the ILC. A possible configuration is to have one IR with a crossing angle of 14 mrad and one with 2 mrad [1]. MAD SURVEY file of the extraction beam optics was used to model the magnet locations, strengths, and orientations in GEANT [2]. Simulated disrupted beams from e^+e^- collisions for the ILC were transported using GEANT [2] in the extraction lines for the 2mrad and 14 mrad crossing angle interaction regions. Particle interactions are simulated in GEANT, and the secondary particles are transported through the extraction line. Magnets apertures, collimators and the beam pipe are simulated. Distributions of positions, energy and angles at (i) the middle of the Energy Chicane, (ii) at the Compton IP for the measurement of polarization and (iii) at the Compton Detector Plane are shown. It is important to have small beam, energy and polarization losses between the e^+e^- Interaction Point and the Compton Polarimeter in the transport of the disrupted beam in the extraction lines. Beam losses, energy losses due to synchrotron radiation and spin diffusion are shown. Distributions of the synchrotron radiation are shown. A previous study of the comparison of the 2 mrad and 14 mrad extraction lines at 500 GeV center-of-mass collision energy is found in reference 3.

The 14 mrad IR allows the beam to continue straight ahead without bends in the horizontal plane. There are chicanes in the vertical plane for measuring the energy and polarization of the beam as shown in Figure 1. The beam is focused by quadrupoles at the Compton IP located at the center of the Polarimeter Chicane 147.682 meters downstream of the e^+e^- IR. The Energy Chicane is located between ~46m and 73m. Synchrotron radiation bands are generated by wiggler magnets in the horizontal plane when the beam has been directed along + or – 2 mrad by the bends in the vertical plane. Synchrotron radiation detectors are placed above and below the beam at the Compton IP to measure the separation between the horizontal bands and, as a result, the energy of the beam.

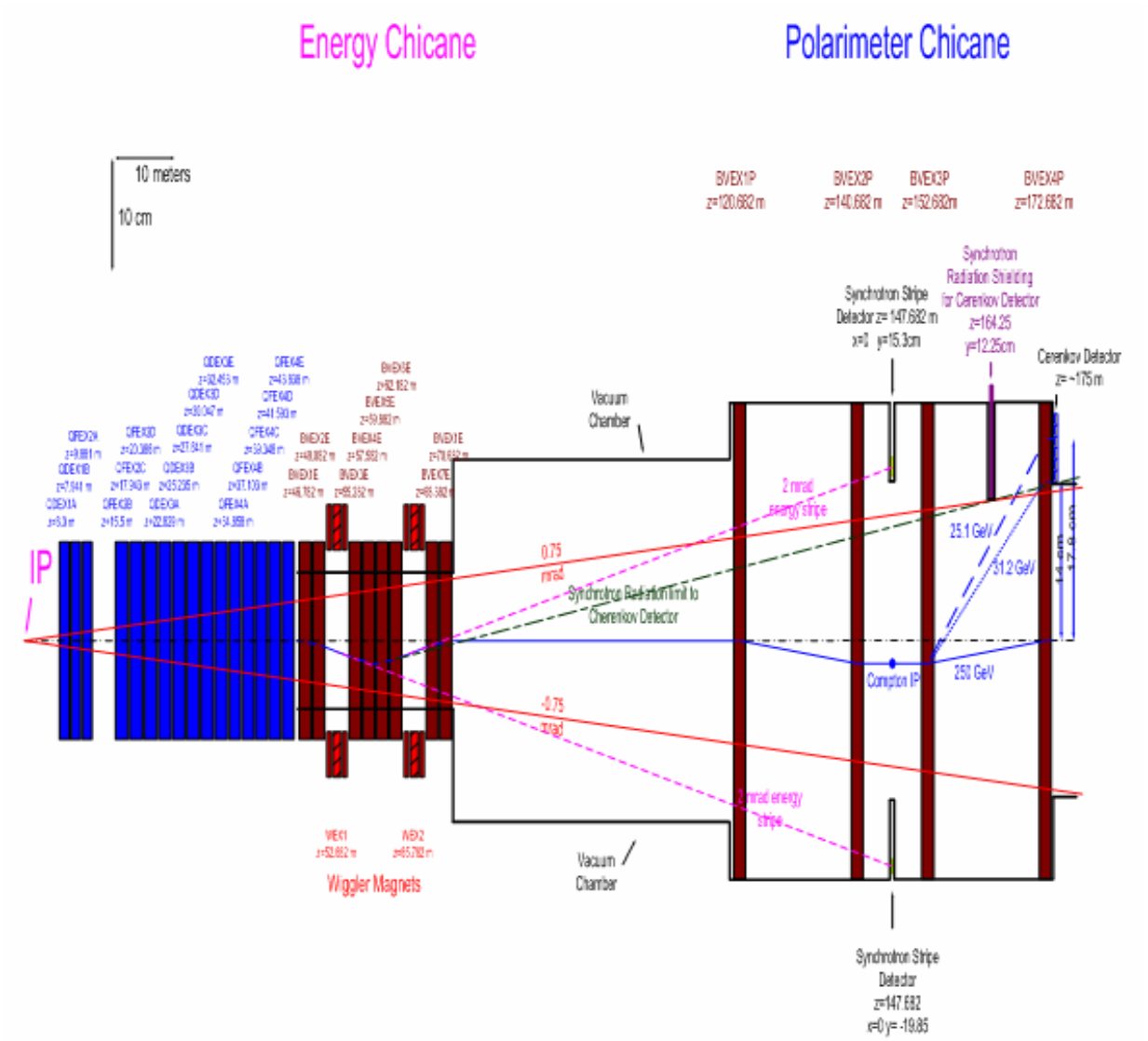

Figure 1: Diagram of the Energy Chicane and Polarimeter Chicane in the 14 mrad extraction line. Longitudinal distances are given from the IP. Also shown is the 0.75 mrad beam stay clear from the IP.

Figure 2 shows a schematic of the 2 mrad extraction line displaying the plan view (top part of figure) and elevation view in the bottom portion of the figure. The 2mrad IR extraction line goes through the final focus quadrupole magnets off axis, and the beam is extracted in the coil pocket of QF1. This is necessary to separate the charged beam from the photons in the beamstrahlung cone of +-0.5 mrad. The low energy beamstrahlung tail of the charged beam is absorbed by a series of collimators in the horizontal and vertical plane embedded in a vertical energy chicane. The Energy Chicane and the Polarimeter

Chicane follow. Just before the Polarimeter Chicane the beam is bent back to the same direction it had at the e^+e^- IR. The direction of the beam at the Compton IP is required to be within 50 micro-radians of that at the e^+e^- IR, so that the polarization is the same as at the e^+e^- IR.

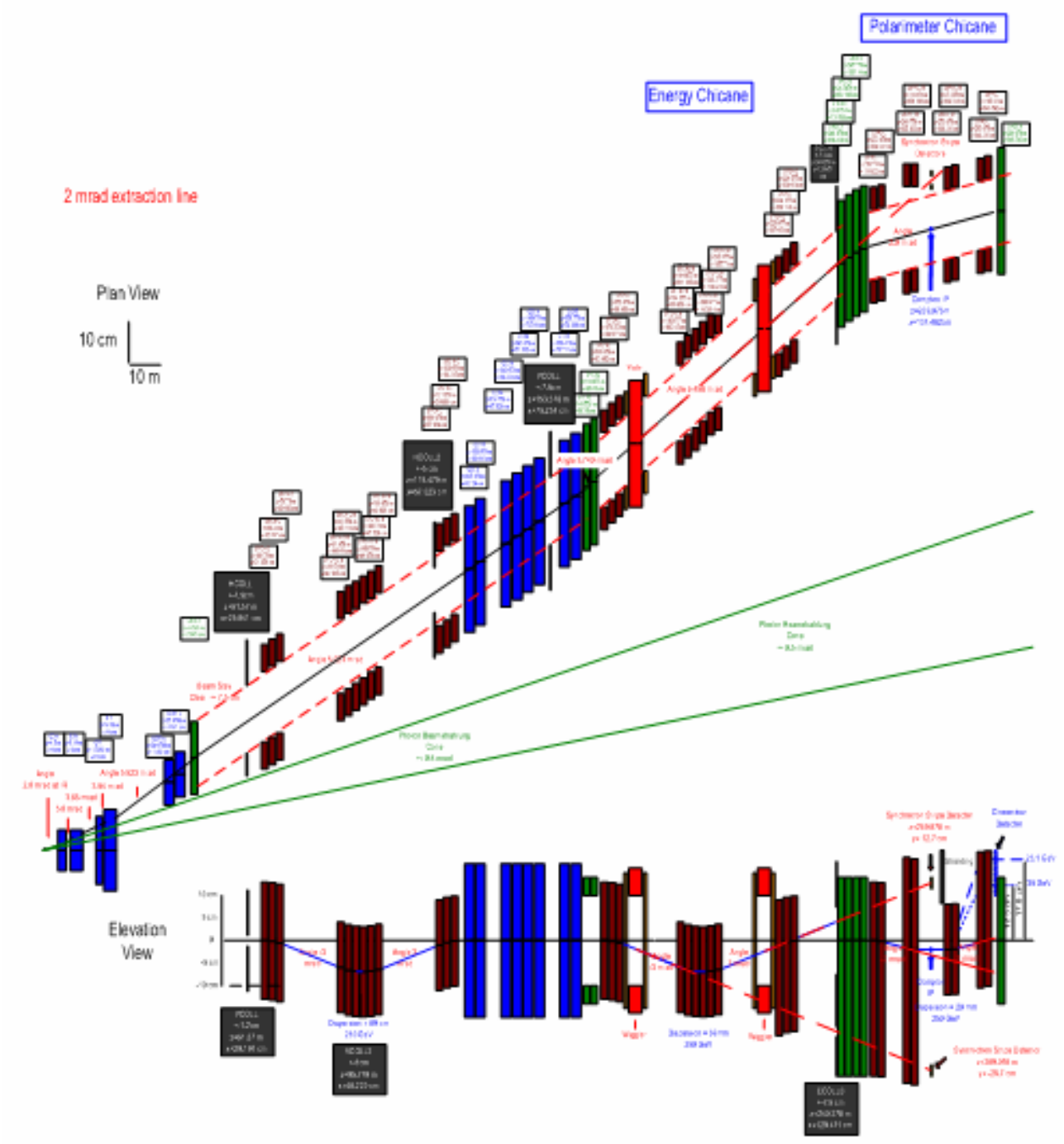

Figure 2: Diagram of the Energy Chicane and Polarimeter Chicane in the 2 mrad extraction line showing the plan view in the upper portion and the elevation view below.

The extraction line transport is simulated using the program GEANT [2]. Disrupted beam events were taken from files prepared by Andrei Seryi [4]. For these studies file cs21 corresponds to a Normal ILC beam with σ_x, σ_y, σ_z of the beam at the interaction region given in Table I. The mean energy and RMS as the beam leaves the IR is also given in Table I. File cs23 has parameters set for Large-y. The Large-y beam parameter data sets with the centroid of the beams missing by 4nm in the vertical and 200nm in the horizontal were also studied. The Low Power beam parameter data set cs24 was studied. The Low Power beam parameter data set achieves similar luminosity as the Normal ILC beam by having a much smaller beam size at the e+e- interaction region and half the number of bunches in each train resulting in larger beamstrahlung. The mean energy of the Low Power beam parameter data set is 440 GeV, and is ~35 GeV lower than the mean energy of the Normal ILC beam parameter data set. The RMS is 74 GeV for the Low Power data set compared to 41 GeV.

Table I: Beam conditions at the e+e- interaction region for the files used in the study. The mean energy and RMS is given for the beam as it leaves the interaction region.

Name	**File**	**σ_x (nm)**	**σ_y (nm)**	**σ_z (nm)**	**E (Mean) (GeV)**	**E (RMS) (GeV)**
Normal ILC	cs21	554	3.5	300	475.5	40.72
Large-y	cs23	367	7	600	463.0	47.54
Large-y dy=4nm	cs23_dy4				461.5	48.23
Large-y dx=200nm	cs23_dx200				464.4	46.38
Low Power	cs24	350	2.7	200	439.6	73.94

Figure 3 shows a plot generated by GEANT giving the magnets and ray traces for 50 beam particles from parameter set cs21. Figure 4 shows the energy distribution for the normal ILC beam parameters, cs21. Figure 5 shows the angular distributions of the disrupted beams for the different beam parameter sets as they leave the e^+e^- IR.

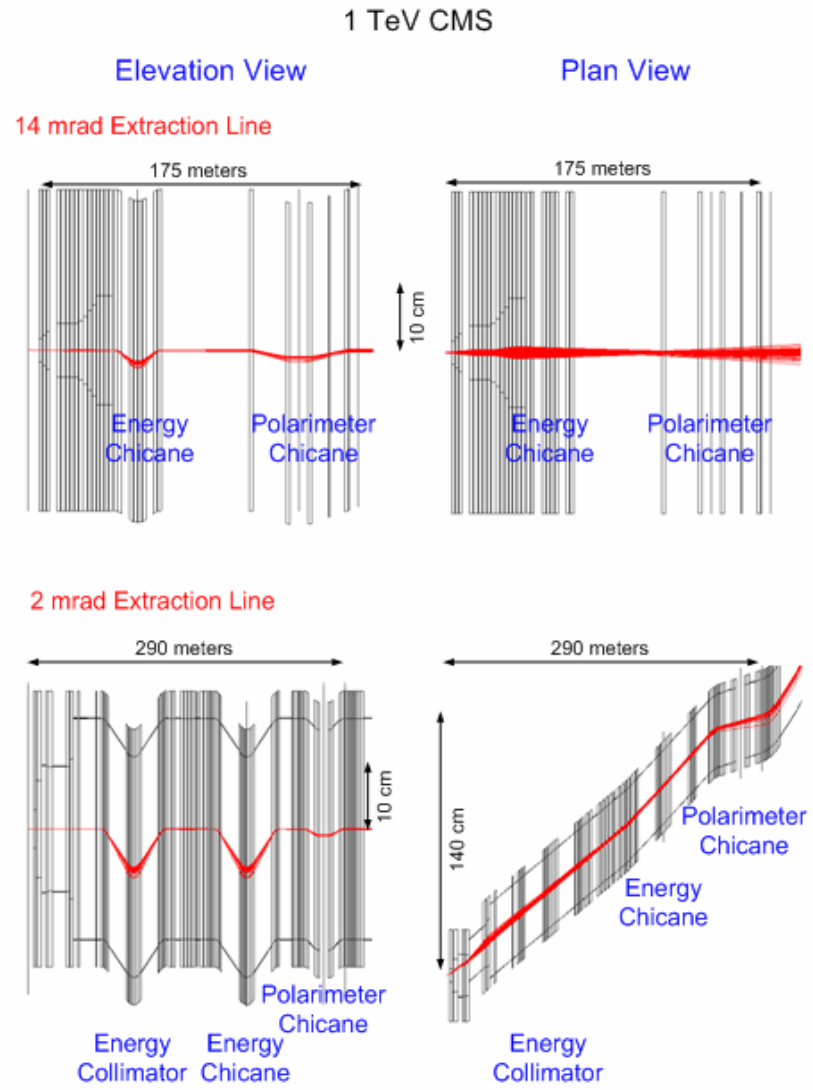

Figure 3: GEANT generated drawing of the beam line elements with 50 beam tracks shown.

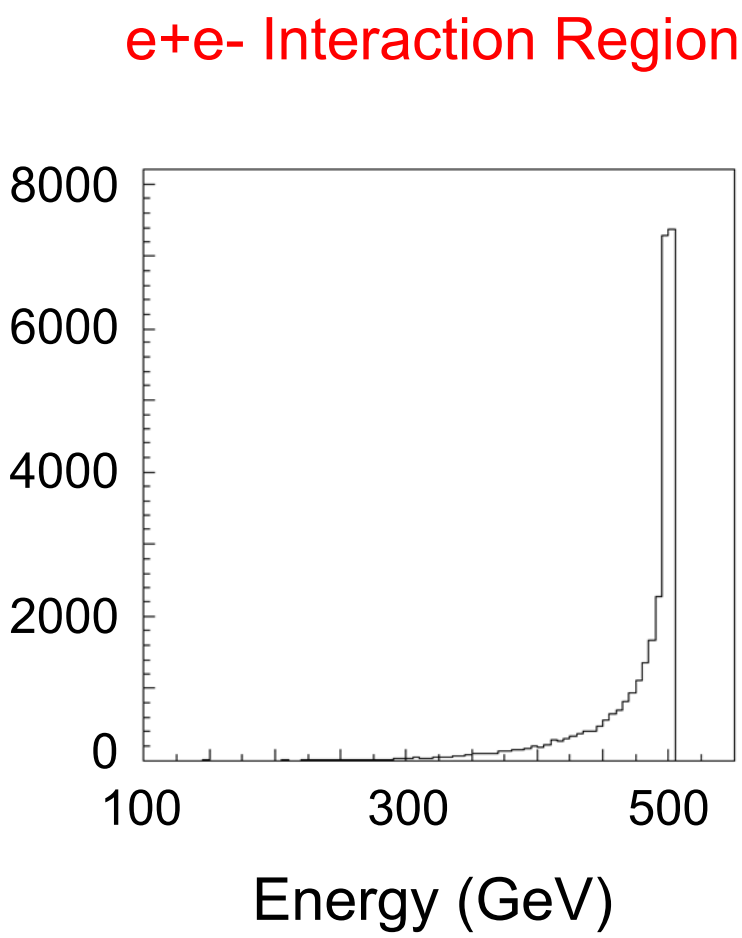

Figure 4: Energy distribution at the e+e- interaction region after collision for cs21 data set corresponding to a 1 TeV CMS Normal ILC beam [4].

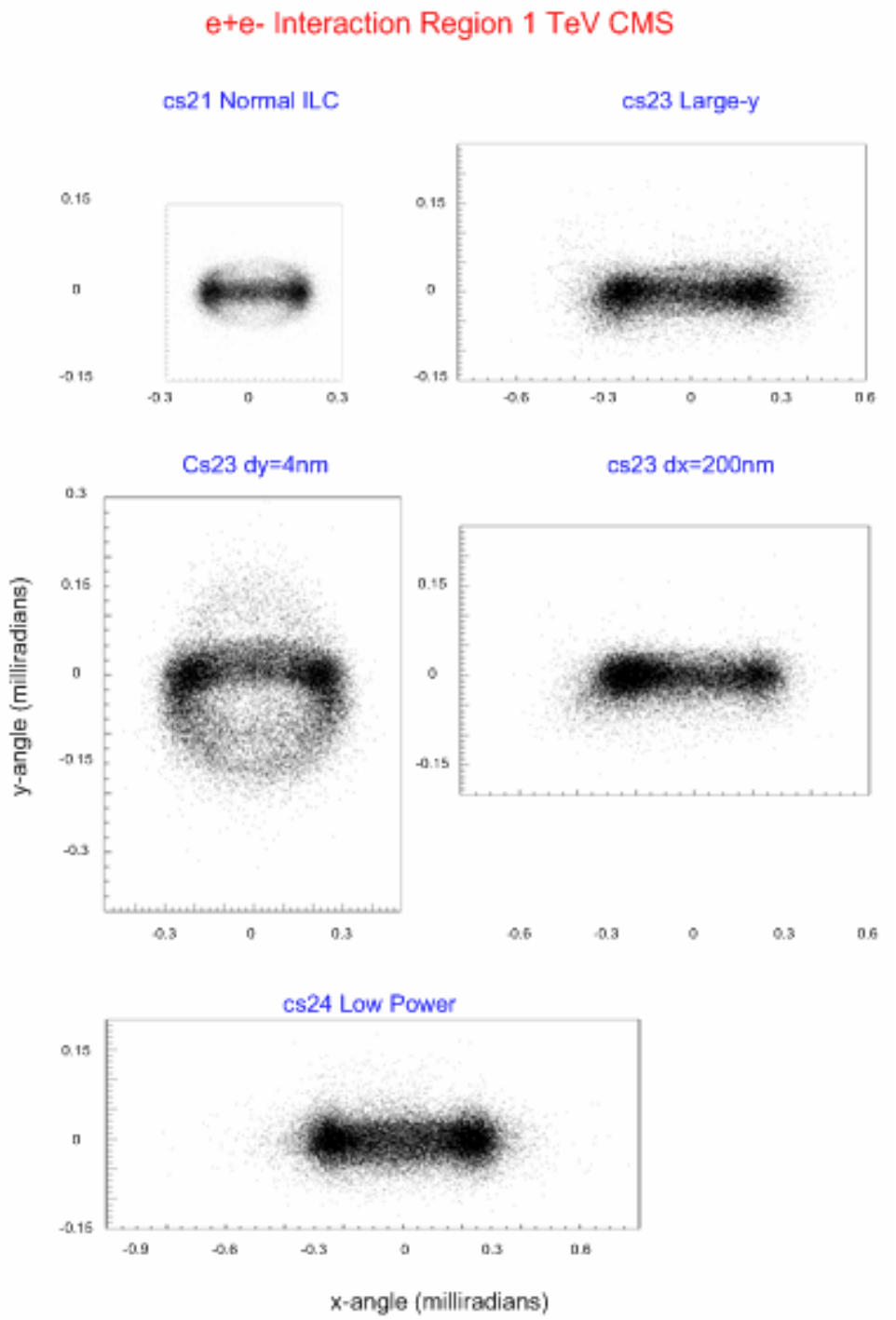

Figure 5: Angular distribution at the e+e- interaction region after collision for different data sets at 1 TeV CMS.

Beam distributions at the Compton IP are shown in figure 6. The dispersion at the Compton IP for a 500 GeV beam particle is 1cm. At 250 GeV the dispersion is 2cm. The

current in the magnets of the polarimeter chicane are the same independent of beam energy so that the positions of the backscattered Compton electrons in the Cherenkov detector are at the same vertical displacement. The vertical position of the laser light is adjusted to collide with the electron beam. The tails of the beam spatial distributions and angular distributions are broader for the 2 mrad extraction line. The beam core distributions are also broader as seen in figure 7.

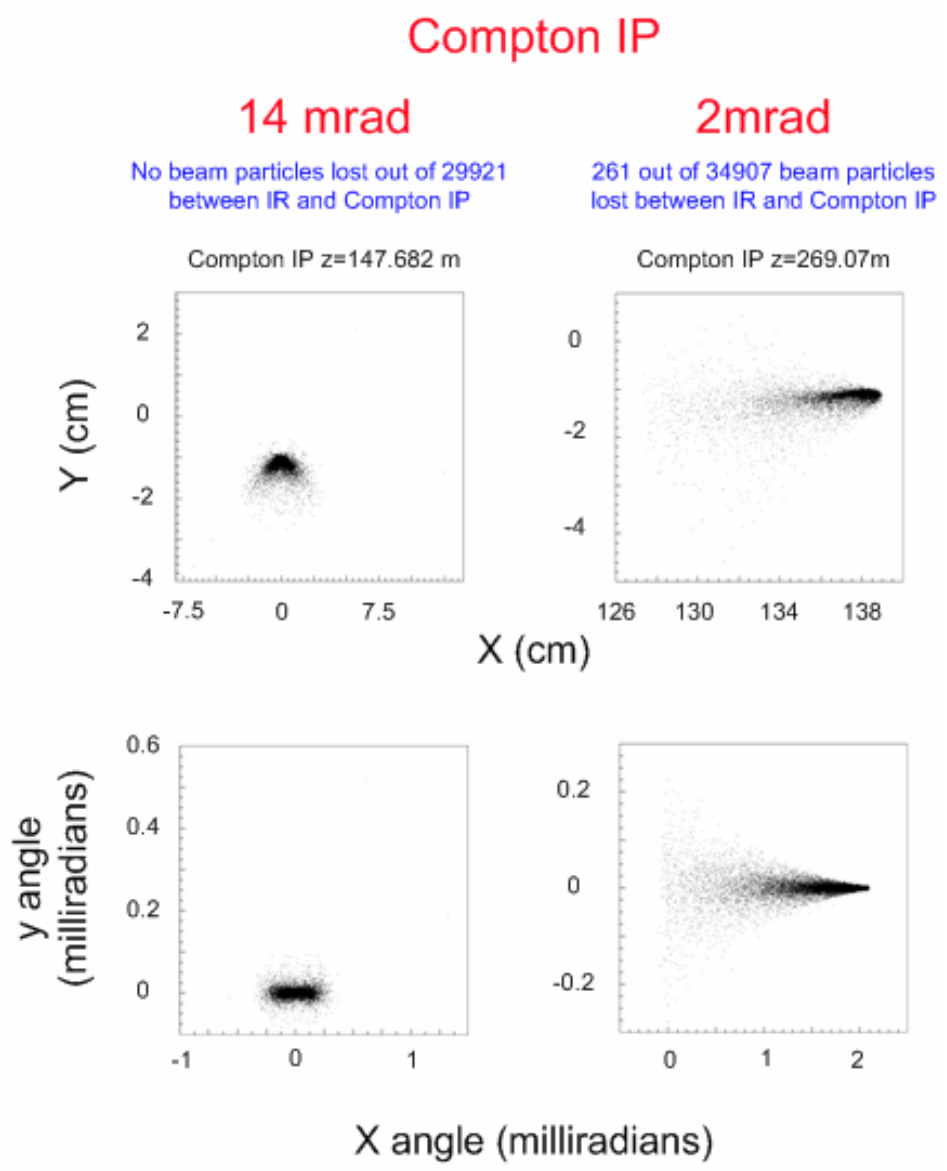

Figure 6: Distribution of y versus x and beam angles at the Compton IP for the 14 mrad and 2 mrad extraction lines. The dispersion at the Compton IP for beam particles at 500 GeV is -1cm.

2. Beam Distributions Contained within Laser Spot Size

The beam is more diffuse at the Compton IP in the 2mrad extraction line than in the 14 mrad extraction line. This is seen in figure 7 where the distribution in x and y are given for those beam tracks within +/-100 microns of the peak. This corresponds to about the size of the laser spot at the Compton IP. The Compton luminosity is more than two times larger in the 14mrad extraction line than that of the 2mrad where the laser light sees only 18.9% of the beam.

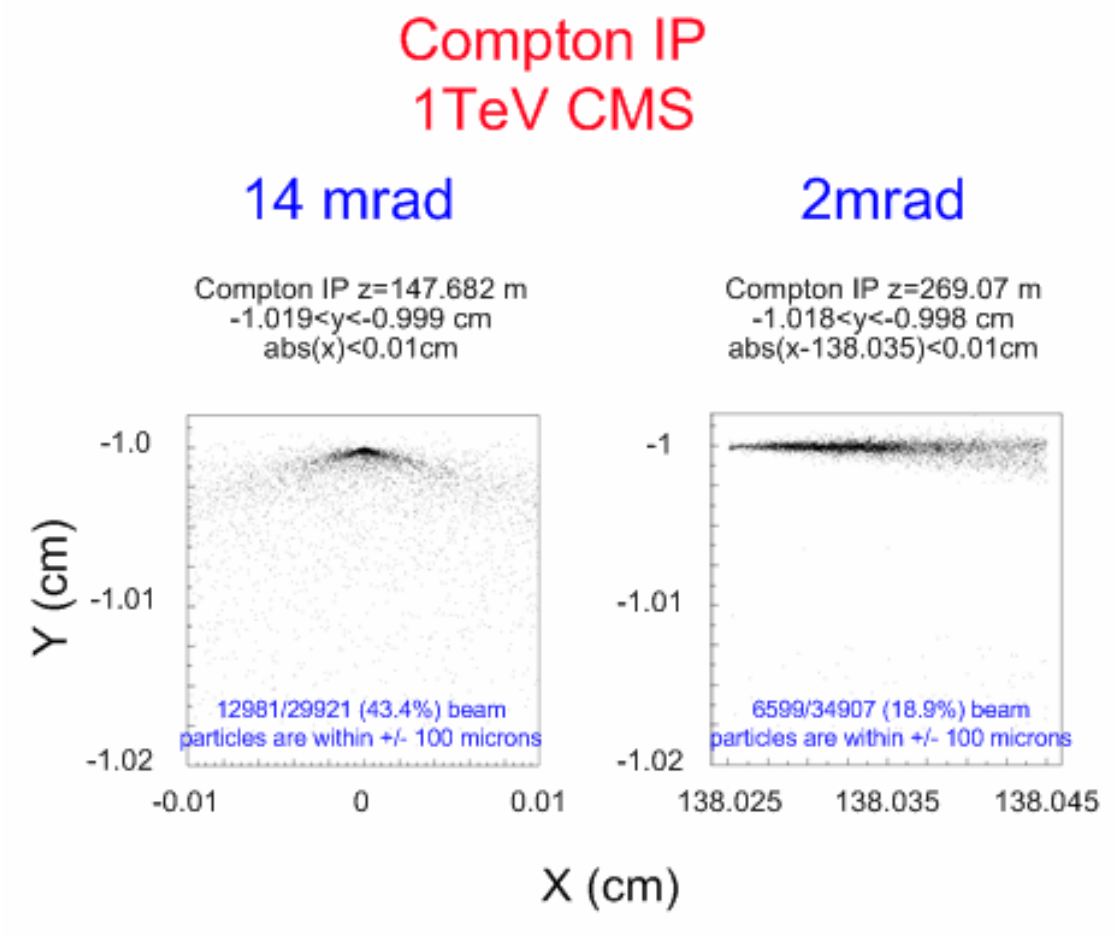

Figure 7: Distribution of y versus x within 100 microns of the peak at the Compton IP for the 14 mrad and 2 mrad extraction lines. The dispersion at the Compton IP for particles of energy 500 GeV is -1cm.

Spin Diffusion depolarization comes from classical (Bargmann-Michel-Telegdi precession: BMT) [5]. BMT spin precession with respect to the electron momentum vector is given by:

$$\theta_{spin} = \gamma \frac{g-2}{2} \cdot \theta_{bend} = \frac{E(GeV)}{0.44065} \cdot \theta_{bend} \qquad (1)$$

As seen in Figure 8 the x-angle distribution at the Compton IP is contained within +-0.2 milli-radians about the direction of the beam at the e+e- collision point. The y-angle distribution is much narrower than the x-angle distribution and does not contribute appreciable to the spin diffusion (see figure 6). Figure 8 also shows the distribution of $P=\cos\theta_{spin}$ at the Compton IP. The tail going down to $\cos\theta_{spin} = 0.96$ shown in the insert of figure 8d for the 2 mrad extraction line data has been included in the mean value of the polarization projection. The mean polarization projection is 99.81% for the 14mrad extraction line and 99.81% for the 2 mrad extraction line distribution.

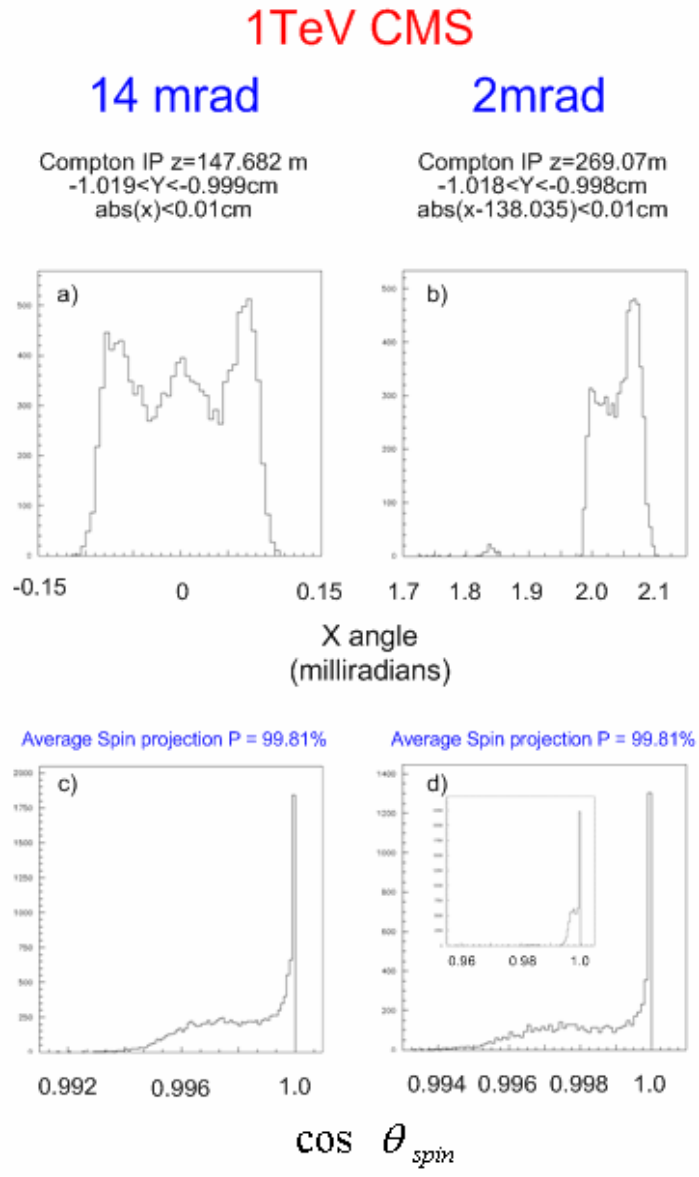

Figure 8: Angular distribution and $P=\cos\theta_{spin}$ for beam particles within 100 microns of the peak at the Compton IP for the 14 mrad and 2 mrad extraction lines. The insert in d) shows the full distribution with no selection. The angle θ_{spin} is given by equation 1.

The polarization at the Compton IP should be compared to the luminosity weighted polarization at the IR, which is approximated by:

$$P_{Luminosity Weighted} = Cos\left(\theta_{SpinLuminosity Weighted}\right) = Cos\left(\frac{E(GeV)}{0.44065}\cdot\frac{1}{2}\theta^{IR}_{x-angle}\right) \quad (2)$$

where $\theta^{IR}_{x-angle}$ is the x-angle of the beam as it leaves the e+e- interaction region. As seen in Figures 5 the y-angle distribution at the IR is much narrower than the x-angle distribution and does not contribute appreciable to the spin diffusion. The optics of the extraction lines were chosen to have R_{12} =-0.5 so that the polarization at the Compton IP is close to the luminosity weighted polarization. The polarization projection at the Compton IP is in excellent agreement with the luminosity weighted polarization of 99.80 % determined from equation 2 confirming the choice of optics in the extraction line. Note that the beam direction as defined in this GEANT study is 2mrad at the Compton IP for the 2 mrad IR extraction line, and this has been subtracted from the angular distribution before taking the spin projection.

The primary polarimeter measurement at the ILC will be performed by a Compton polarimeter. An accuracy of (Pe^+=Pe^-) = 0.25% should be achievable [6]. Polarization measurements with collider data may reach an accuracy of 0.1% [6].

Table II gives the accepted beam and average polarization projection for various +-100 micron selections about the x value of the beam at the Compton IP for the 2 mrad extraction line. The laser spot size at the Compton IP is about 100 microns. Polarization varies by 0.16% and the Compton luminosity decreases by a factor of two when moving off the peak by 0.6 mm. As can be seen in Figure 7 the x and y distributions fall off rapidly for the 14 mrad extraction line and only a few percent of the beam remains when stepping away from the peak.

Table II: 2mrad Extraction Line: Beam accepted and polarization projection for various +- 100 micron selections about the x' value of the beam at the Compton IP. In each case -1.998<y<-0.998cm and abs(x-x')<0.01cm. Normal ILC beam parameter data set used.

x' +- 100 microns	%Beam within +-100microns in x & y	Luminosity Weighted Polarization at the IR	Polarization Projection
138.035	18.9	99.80 %	99.81 %
138.055	8.5	99.80 %	99.82 %
138.075	11.5	99.80 %	99.67 %
138.095	8.8	99.80 %	99.66 %

Table III gives the beam accepted within +-100 micro-meters about the peak at the Compton IP for different beam conditions at the e^+e^- IR. The Compton Luminosity varies by <30% when the beam collisions are offset by 200 microns in the horizontal and 4 microns in the vertical. The Compton Luminosity decreases by ~2 from the Nominal

ILC beam parameter data set to the Large-y and the Low Power beam parameter data sets.

The luminosity weighted polarization and the polarization projection at the Compton IP are also shown in Table III for the different data sets. The luminosity weighted polarization changes by 0.47 % between the Normal ILC beam parameter data set and the Low Power beam parameter data set. The Large-y and Low Power beam parameter data sets show small variation (less than 0.21%) between the polarization at the Compton IP and the luminosity weighted polarization. The polarization measurement at the Compton IP should be within the desired precision of +- 0.25% for both the 2mrad and the 14 mrad extraction lines.

Table III: Beam accepted within +-100 micro-meters about the peak and polarization projection for different data sets at the Compton IP.

A) 14mrad Extraction Line with -1.019<y<-0.999cm and abs(x)<0.01cm:

Condition (file name)	**%Beam within +-100microns in x & y**	**Luminosity Weighted Polarization at the IR**	**Polarization Projection at the Compton IP**
Normal ILC Beam Condition (cs21)	43.4 %	99.80 %	99.81 %
Large y (cs23)	23.2 %	99.43 %	99.55 %
Large y horizontal offset 200nm (cs23_dx200)	24.1 %	99.33 %	99.54 %
Large y vertical offset 4nm (cs23_dy4)	20.7 %	99.43 %	99.55 %
Low Power (cs24)	22.7 %	99.50 %	99.55 %

B) 2 mrad Extraction Line with -1.998<y<-0.998:

Condition (file name)	**%Beam within +-100microns in x & y**	**Luminosity Weighted Polarization at the IR**	**Polarization Projection at the Compton IP**
Normal ILC Beam Condition (cs21) **abs(x-138.035)<0.01cm**	18.9 %	99.80 %	99.81 %
Large y (cs23) **abs(x-138.041)<0.01cm**	7.3 %	99.43 %	99.62 %
Large y horizontal offset 200nm (cs23_dx200) **abs(x-138.041)<0.01cm**	9.8 %	99.33 %	99.20 %
Large y vertical offset 4nm (cs23_dy4) **abs(x-138.040)<0.01cm**	7.8 %	99.43 %	99.27 %
Low Power (cs24) **abs(x-138.039)<0.01cm**	7.3 %	99.50 %	99.68 %

3. Beam Losses

Beam losses between the e^+e^- Interaction Region and the Compton Detector Plane are given in Table IV. Beam losses of ~$1.0 * 10^{-4}$ occur in the 14 mrad extraction line for the Normal ILC Beam Condition parameter set (cs21) and the Large-y parameter set (cs23). The Low Power parameter set (cs24) has larger losses of 0.53% and produces significant background in the region of the Cherenkov detector. There is an estimated $8.6 * 10^4$ photons per cm^2 in the Cherenkov detector with half having energy above Cherenkov threshold of ~10 MeV. This will pose a serious background in the Cherenkov detector and will require collimators be installed between the e+e- IR and the Compton IP or an increase in the beam stay clear from the present 0.75 mrad.

The 2 mrad extraction line has been designed with collimation to absorb losses at specific places along the extraction line. Around one percent of the beam is lost in the 2 mrad extraction for the Normal beam and Large-y beam parameter data sets. The Low Power beam parameter data set has 7.3 % beam losses between the e+e- IR and the Compton detector plane. There is an estimated $1.1 * 10^4$ photons per cm^2 in the Cherenkov detector for the Low Power beam parameter data set. Half of these have energy above Cherenkov threshold of ~10 MeV. This will pose a serious background in the Cherenkov detector. However, losing more than one percent of the beam on the collimators and distributed along the 2 mrad extraction line will give serious radiation issues.

Table IV: Beam Losses from the e+e- IR to the Compton Detector Plane at 1TeV CMS.

a) 14 mrad Crossing Angle Extraction Line

Condition (file name)	**Losses**	**Beam**	**Lost Beam**
Normal ILC Beam Condition (cs21)	0	29921	$<0.6 * 10^{-4}$
Large y (cs23)	3	29916	$1.0 * 10^{-4}$
Large y horizontal offset 200nm (cs23_dx200)	2	29918	$0.7 * 10^{-4}$
Large y vertical offset 4nm (cs23_dy4)	3	29928	$1.0 * 10^{-4}$
Low Power (cs24)	186	34905	0.53 %

b) 2 mrad Crossing Angle Extraction Line

Condition (file name)	**Losses**	**Beam**	**Lost Beam**
Normal ILC Beam Condition (cs21)	261	34907	0.75 %
Large y (cs23)	494	34901	1.42 %
Large y horizontal offset 200nm (cs23_dx200)	355	34904	1.02 %
Large y vertical offset 4nm (cs23_dy4)	507	34915	1.45 %
Low Power (cs24)	2545	34905	7.29 %

Beam losses for the normal beam parameters were studied with a larger sample by using a file generated containing only the tails of the disrupted beam having disrupted beam with energy less than 0.65 of the 500 GeV beam energy or the angle greater than 0.5 mrad:

http://www.slac.stanford.edu/~seryi/ILC_new_gp_files/cs21_hs/tail1_lt_0_65E0_or_gt_500urad.dat

Figure 9 shows the energy and angular distributions of the tail file beam tracks as they leave the e+e- IR.

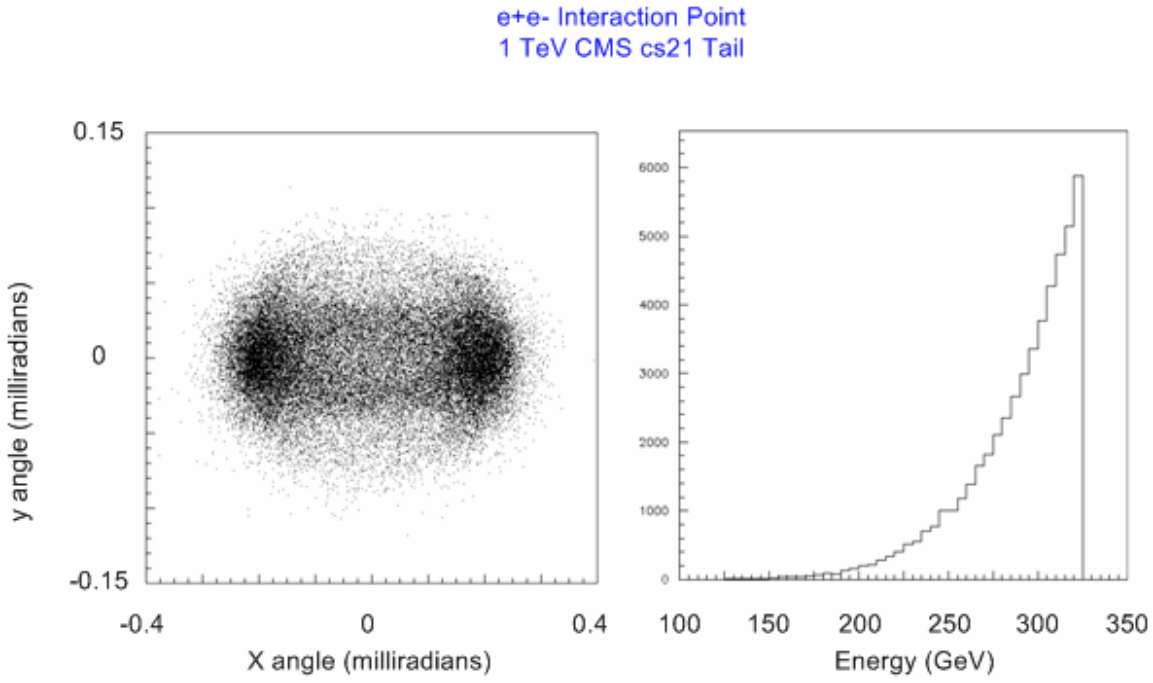

Figure 9: Normal ILC beam parameter data set tail sample angular and energy distributions at the e+e- interaction point for outgoing beam particle with energy less than 0.65 of the incoming beam energy or angles greater than 0.5 mrad.

There are 57 particles from this 40,000 Normal ILC beam tail sample lost between the IR and the Compton detector plane in the 14 mrad extraction line. This represents a loss of $1.8*10^{-5}$ of the 3.2 million original beam tracks. Figure 10 shows the x and y distributions at the Compton Detector plane. There is no background from this Normal ILC beam parameter data set in the region of the Compton Cherenkov detector from charged or neutral particles ($<50/cm^2$).

The 2 mrad extraction line has large losses of the beam mainly on the collimators in the extraction line. There are 28,263 beam tracks lost between the e+e- IR and the Compton Detector plane from the 50,000 beam tracks used from the tail file of the Normal ILC beam parameter data set. This represents a loss of 0.72% of the 3.92 million original beam tracks used to produce the tail file sample used in this study. Figure 10 shows the x and y distributions at the Compton Detector plane. There is background in

the region of the Compton Cherenkov Detector coming mainly from secondary photons. From this study we estimate ~460 photons/cm^2 are in the region of the Cherenkov counter cells for each bunch of 2*10^{10} electrons. The spectra of the background photons are mainly below Cherenkov threshold of ~10 MeV. The Compton scattered electron signal is ~1000/cm^2 at the endpoint of the backscattered electron energy. For the Normal ILC beam parameter data set the background at the Compton detector from lost beam particles should be small compared to the signal.

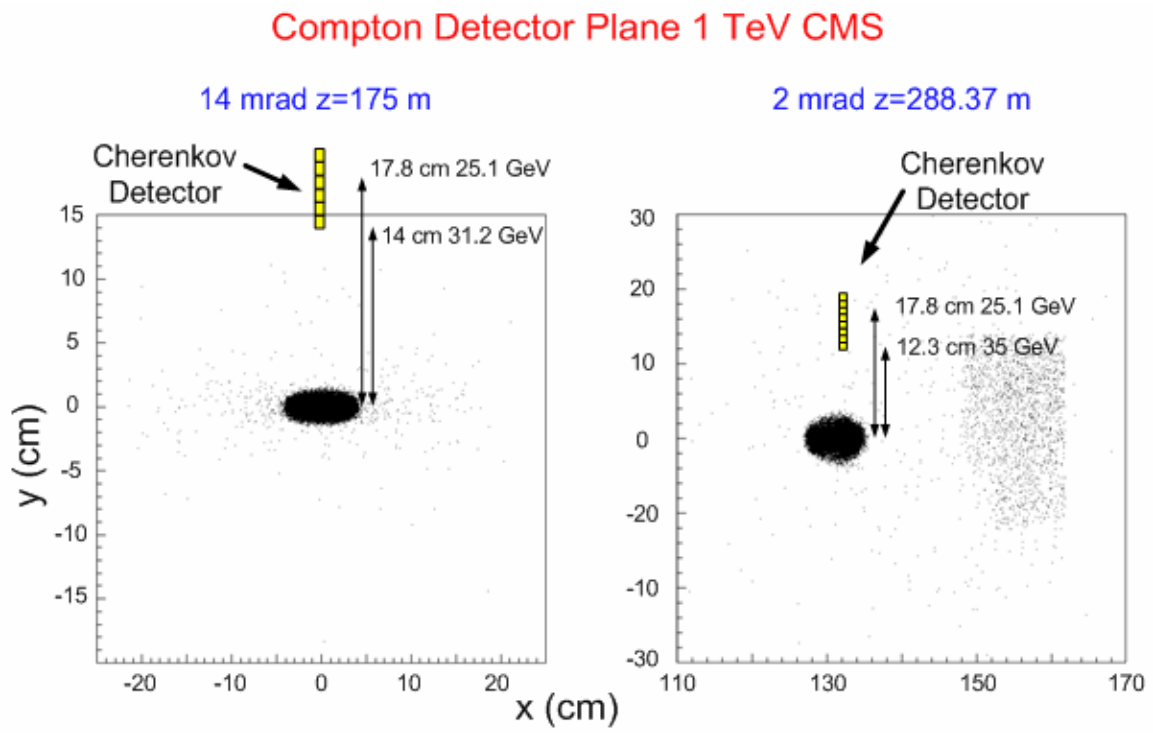

Figure 10: The horizontal and vertical distributions of the beam particles and background produced at the Compton Detector plane from the lost beam particles of the tail sample from the Normal ILC beam parameter data set.

4. Synchrotron Radiation

Synchrotron radiation produced in the bends and quadrupole magnets is shown by the blue rays in figure 11. Due to the horizontal bends and the energy collimator chicane in the 2 mrad extraction more synchrotron radiation is generated.

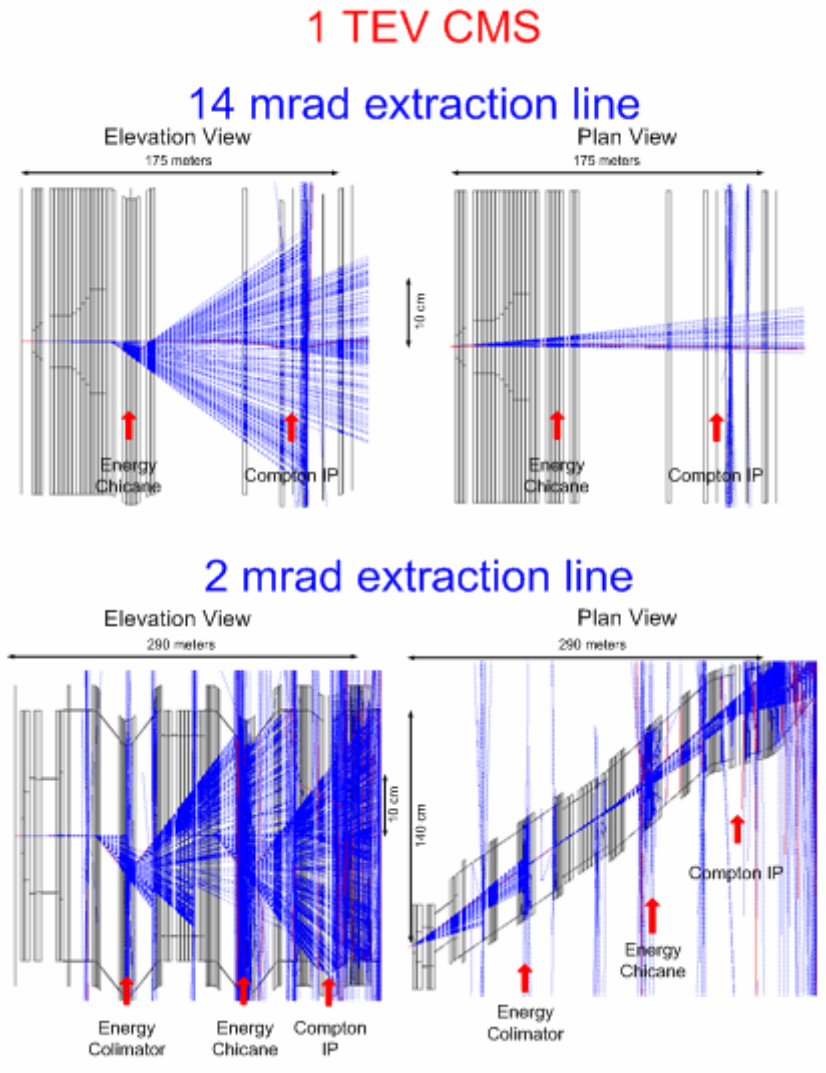

Figure 11: Synchrotron radiation in the 14 mrad and 2 mrad extraction lines. The rays colored blue are the synchrotron radiation rays.

Figure 12 shows the beam energy of the Normal ILC parameter data set at the (a) e+e- interaction region and at the middle of the energy spectrometer for the (b) 14 mrad and (c) 2 mrad extraction lines. At the e+e- interaction point there is a long beamstrahlung tail with about a fourth of the beam in the peak at 500 GeV. Synchrotron radiation losses in the magnets between the IR and the center of the energy chicane broaden the peak and shift it to a lower energy. Beam energy losses due to synchrotron radiation are shown in (d) and (e) of Figure 12 where the difference between the energy of the beam at the IR and the beam energy at the middle of the energy chicane is given. The energy spectrometer will measure the distributions given in (b) and (c) of figure 12.

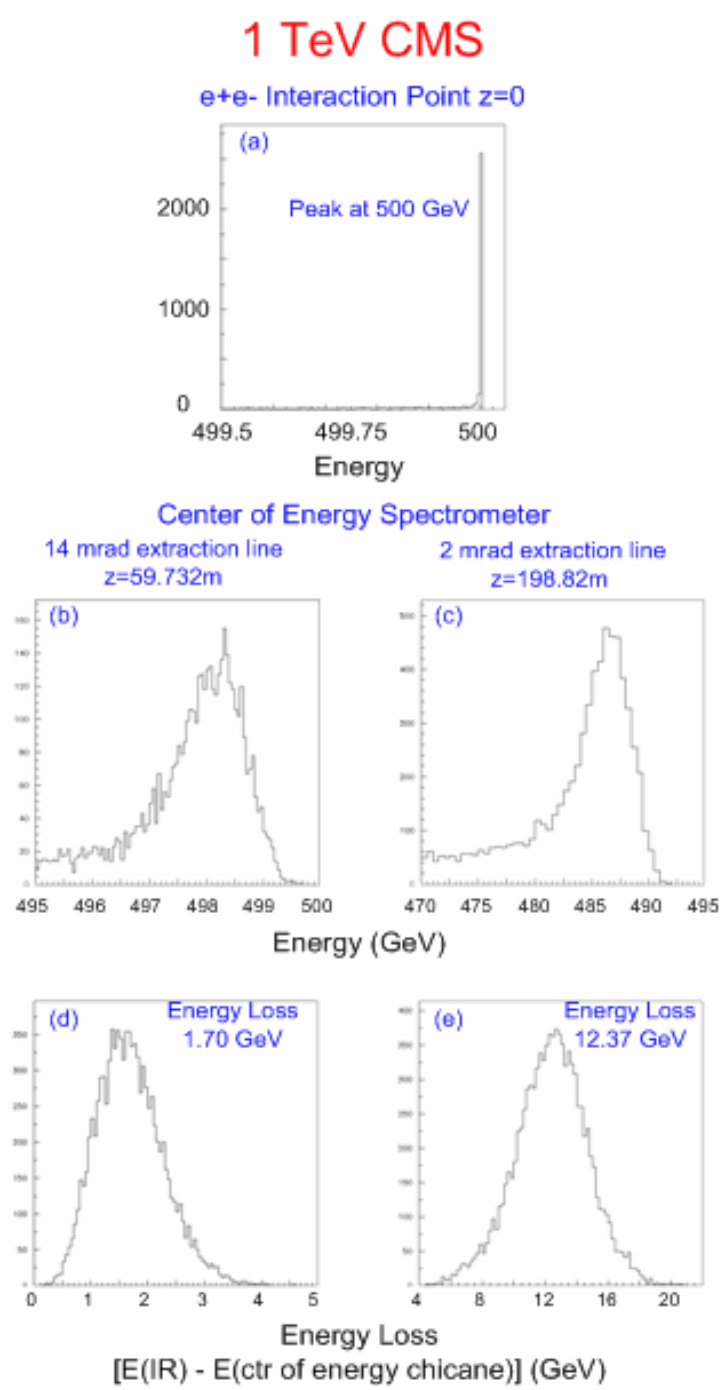

Figure 12: Energy of the disrupted beam at the (a) e+e- interaction region and at the center of the energy spectrometer for the (b) 14 mrad (z=59.732m) and (c) 2 mrad (z=198.82m) extraction lines. The lower energy of the peak is due to synchrotron radiation losses in the magnets. In (d) and (e) the difference between the energy of the beam at the interaction region and the middle of the energy chicane is shown.

The energy loss between the Interaction Region and the center of the energy chicane is given in Table V for the different disrupted beam parameter sets. An energy loss of 1.70 GeV occurs in the 14 mrad extraction line with variation between beam parameter data sets of 160 MeV. The 2 mrad extraction line has a loss of 12.4 GeV and the variation between beam parameter data sets is 750 MeV. The variation in energy loss due to synchrotron radiation is large.

It is important to know the energy of the beam at the e+e- interaction point to a precision of 100 ppm (~50 MeV at 500 GeV beam energy) [8]. The synchrotron radiation losses between the e+e- interaction point and the energy spectrometer in the 2 mrad extraction line have variations fifteen times larger than the desired precision depending on the beam parameters. The variations in the 14 mrad extraction line are 3 times larger than the desired precision.

The variation in energy loss due to synchrotron radiation can come from different causes: a) For beam parameter data sets with large beamstrahlung the energy spectrum is shifted to lower energy and will radiated less synchrotron radiation as they traverse the magnets between the IR and the energy chicane since the synchrotron radiation goes as E^2. b) The beam may take different paths through the extraction line and experience different magnetic fields. Situation b) could occur in the 2 mrad extraction line since the beam goes through quadrupoles off axis.

Table V also gives the synchrotron radiation energy loss for beam particles with E>480 GeV. The large variations should be reduced if it is caused by a broader energy spectrum. The variation between beam parameter data sets near the beam energy is only ~40 MeV in the 14 mrad extraction line, and indicates that the lower energy loss in the Low Power beam parameter data set is due to the large beamstrahlung broadening the energy spectrum. Measuring the high energy part of the beam energy spectrum in the 14 mrad extraction line should allow the energy loss due to synchrotron radiation to be understood to the precision required.

The two effects contribute to the 2 mrad extraction line for the Large-y with 200nm horizontal offset beam parameter data set. Even selecting beam particles with E>480GeV the beam energy loss is 450 MeV lower than the other beam parameter data sets. This means that horizontal jitter in the beam collisions at the e+e- IR will give large changes in the energy at the energy spectrometer due to variation in the amount of synchrotron radiation loss in the path of the beam through the quadrupoles. The collision offset data from instruments near the e+e- interaction region can be used to reduce the uncertainty in the synchrotron radiation loss due to horizontal jitter. Its impact on the systematic errors for the energy measurement in the 2 mrad extraction line at 1TeV CMS needs further study.

Table V: Energy Loss from Synchrotron Radiation between the e+e- IR and the Center of the Energy Chicane at 1TeV CMS.

a) 14 mrad Crossing Angle Extraction Line

Condition (file name)	Energy Loss (GeV)	Energy Loss (GeV) for E>480 GeV
Normal ILC Beam Condition (cs21)	1.70	1.83
Large-y (cs23)	1.71	1.86
Large-y horizontal offset 200nm (cs23_dx200)	1.72	1.87
Large-y vertical offset 4nm (cs23_dy4)	1.70	1.85
Low Power (cs24)	1.56	1.87

b) 2 mrad Crossing Angle Extraction Line

Condition (file name)	Energy Loss (GeV)	Energy Loss (GeV) for E>480 GeV
Normal ILC Beam Condition (cs21)	12.37	13.13
Large-y (cs23)	12.16	13.08
Large-y horizontal offset 200nm (cs23_dx200)	11.75	12.71
Large-y vertical offset 4nm (cs23_dy4)	12.04	12.99
Low Power (cs24)	11.62	13.16

The x vs. y distribution of the synchrotron radiation at the Compton IP is shown in figure 13. The location of the synchrotron radiation from the wigglers is shown by the yellow bars (synchrotron radiation from the wigglers is not simulated in this study). The horizontal offset seen in the 2 mrad extraction line is due to the horizontal bend between the energy spectrometer and the Compton IP. The strength of the wiggler bend angle will be chosen so that the synchrotron radiation stripe detectors will not be sensitive to most of the background from the main bend stripe, and good signal to noise will be achievable.

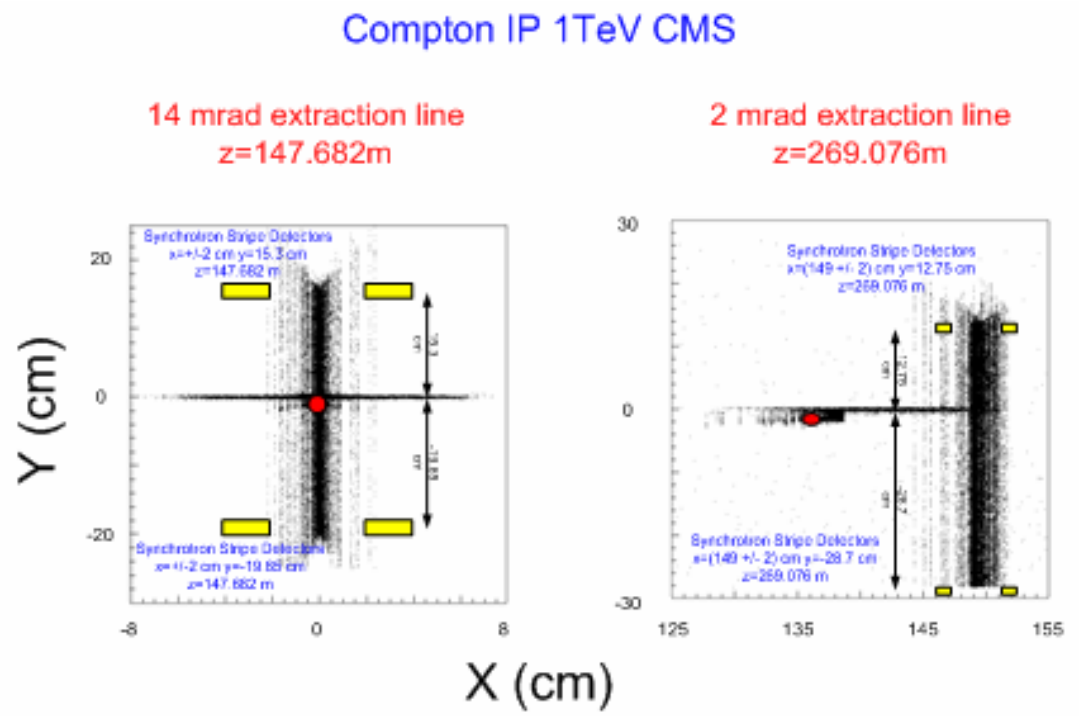

Figure 13: The x vs. y distribution of the synchrotron radiation at the Compton IP for the 14 mrad extraction line and the 2 mrad extraction line. The yellow bars show the location of the detectors to measure the synchrotron radiation from the wigglers of the energy spectrometer (not generated in this GEANT study).

The synchrotron radiation is shown in figure 14 at the location of the Compton Detector. Due to the horizontal bends in the 2 mrad extraction line the Compton detector does not see the direct synchrotron radiation from the upstream magnets. However, the scattered synchrotron radiation background is very large in the region of the Cherenkov detector giving an estimate of $1.6*10^6$ photons/cm^2 per $2*10^{10}$ electrons with photon energy above 15 MeV. This large background may be reduced by careful design of the collimators and shielding of the Cherenkov detector.

The 14 mrad extraction line is different. A collimator is placed at z=164.25m to intercept the synchrotron radiation (see figure 2). As seen in figure 14 the first Cherenkov cell beginning at y~14 cm does not see the direct synchrotron radiation, which is below 13.7 cm. It may be necessary to begin the first Cherenkov cell higher than 14 cm or extend the collimator at z~164.25m slightly inside the 0.75 mrad beam stay clear. Compton backscattered electrons of 31.2 GeV will reach the Compton detector at y=14 cm. Compton scattering at 180 degrees has electron energy of 25.1 GeV and reaches the Compton detector at y=17.8 cm. Four 1 cm Cherenkov cells can cover the range of the Compton scattering between the beam pipe and the kinematic edge. In a study of 10,000 beam tracks at 500 GeV there is estimated $<2*10^4$/cm^2 scattered synchrotron radiation photons with photon energy >15 MeV in the region of the Cherenkov counter from a

single bunch of $2*10^{10}$ electrons. This background may be reduced by careful design of the collimator at z=164.25m and shielding of the Cherenkov detector.

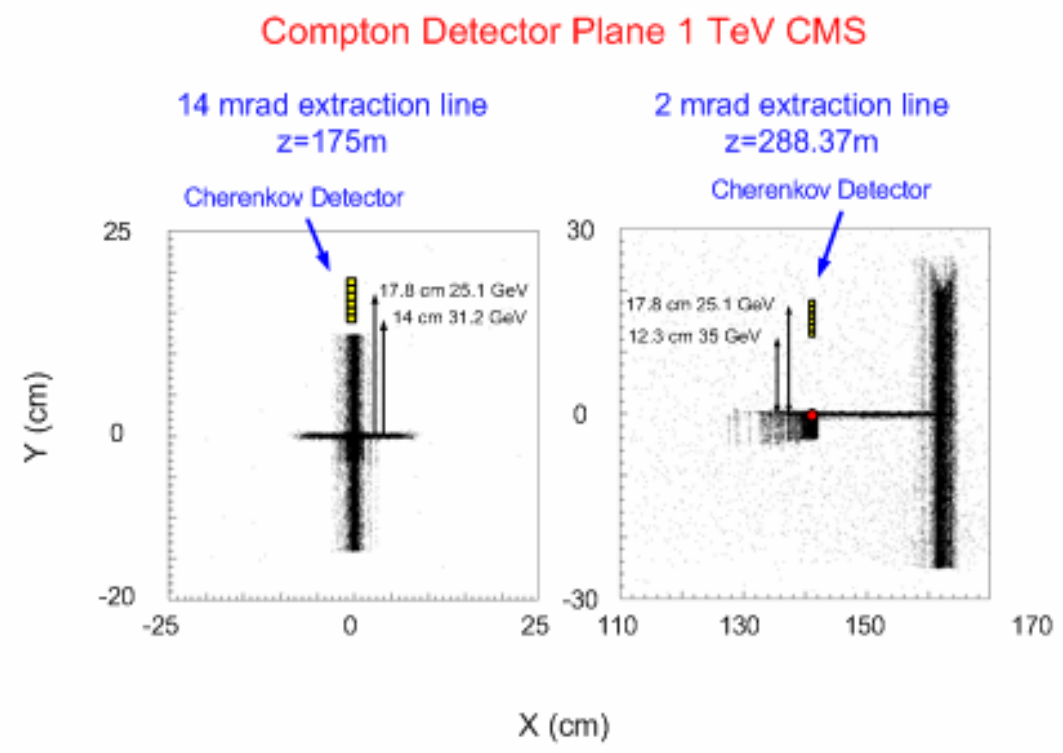

Figure 14: The x vs. y distribution of the synchrotron radiation at the Compton Detector for the 14 mrad extraction line and the 2 mrad extraction line. The yellow bars show the location of the Cherenkov detector.

5. Conclusions for 500 GeV beam energy (1 TeV CMS)

The 14 mrad extraction line:

- At the Compton IP 43% of the beam is contained within +-100microns of the peak giving reasonable luminosity for Compton scattering of the laser light on the disrupted electron beam. The large-y and low power parameter data sets have a lower Compton luminosity by a factor 2.

- The polarization at the Compton IP is in good agreement with the estimated luminosity weighted polarization.

- Beam losses of $1.8*10^{-5}$ occur between the e+e- IR and the Compton detector plane for the Normal ILC beam parameter data set. Beam losses are also small

but not negligible for the Large-y beam parameter data set. There are large losses of 0.53% of the beam for the Low Power beam parameter data set that will require insertion of a new collimator between the e+e- IR and the Compton detector plane or an increase in the beam stay clear from 0.75 mrad.

- Both the Normal ILC and Large-y beam parameter data sets have beam energy losses of ~1.70 GeV due to synchrotron radiation in the magnets between the e+e- IR and the middle of energy chicane with variations less than 20 MeV. The Low Power beam parameter data set has beam energy loss due to synchrotron radiation of 1.56 GeV or 140 MeV less than the other data sets. This is due to the larger beamstrahlung energy tail having smaller synchrotron radiation losses. Measuring the high energy part of the beam energy spectrum will allow the energy loss due to synchrotron radiation to be understood to the precision required.

- The collimator at z=164.25 meters absorbs the synchrotron radiation above the 0.75 mrad beam stay clear allowing the Cherenkov detector to begin at y~14 cm. Background from scattered synchrotron radiation is large at the Cherenkov detector and will require careful design of the collimation and shielding.

The 2 mrad extraction line:

- There are large beam losses between the e+e- IR and the Compton detector plane (0.74% of the beam is lost for the Normal ILC beam parameter data set) giving secondary backgrounds of mainly low energy photons of less than 10 MeV in the region of the Cherenkov Detector. Since the Compton scattered electron signal is large the signal to noise should be favorable for the Normal ILC beam parameter data set. For the Low Power beam parameter data set 7.3% of the beam is lost giving large backgrounds at the Cherenkov detector. Losing more than one percent of the beam in 2 mrad extraction line before the Compton detector plane will give serious radiation issues.

- At the Compton IP only 18.9% of the beam with Normal ILC beam parameters is contained within +-100microns of the peak giving a lower luminosity for Compton scattering of the laser light on the disrupted electron beam.

- The polarization measurement at the Compton IP is within the desired precision of +- 0.25% of the estimated luminosity weighted polarization.

- There are large beam energy losses (12.4 GeV) due to synchrotron radiation between IR and the center of the energy chicane at z=198.82 meters. Beam collision jitter in the horizontal plane of 200 nanometers gives large variations in the beam energy loss due to synchrotron radiation. The collision offset data from instruments near the e+e- interaction region can be used to reduce the uncertainty

in the synchrotron radiation loss due to horizontal jitter. Its impact on the systematic errors for the energy measurement in the 2 mrad extraction line at 1TeV CMS needs further study.

- The detector does not see direct synchrotron radiation from the magnets upstream of the polarimeter chicane. The direct synchrotron radiation from the horizontal bend magnets and polarimeter chicane magnets are below a few centimeters at the Cherenkov detector plane and do not give a background at the Cherenkov detector. However, background from scattered synchrotron radiation is very large at the Cherenkov detector and will require careful design of the collimation and shielding.

References

[1] R. Appleby, Y. Nosochkov, Andrei Seryi et al. Extraction Line Designs for 2mrad and 20mrad IRs, Workshop on Machine-Detector Interface at the International Linear Collider, , Crossing Angle Session, see http://www-conf.slac.stanford.edu/mdi.

Y. Nosochkov, K. Moffeit, A. Seryi, C. Spencer, M. Woods (SLAC), D. Angal-Kalinin, R. Appleby (Daresbury), B. Parker (Brookhaven). Optics of the ILC extraction line for 2 mrad crossing angle. SLAC-PUB-11613, EUROTEV-REPORT-2006-001, SNOWMASS-2005-ILCAW0525, Jan 2006.

Y. Nosochkov, T. Markiewicz, T. Maruyama, A. Seryi (SLAC), B. Parker (Brookhaven). ILC Extraction Line for 14 mrad Crossing Angle. SLAC-PUB-11591, Dec 8, 2005.

[2] GEANT-3, CERN Program Library Long Write-up W5013, CERN, March 1994.

[3] Ken Moffeit, Takashi Maruyama, Yuri Nosochkov, Andrei Seryi and Mike Woods *SLAC,* William P. Oliver *Tufts University,* Eric Torrence *University of Oregon,* Comparison of 2 mrad and 14/20 mrad Crossing Angle Extraction Lines, SLAC-PUB-11956, July 2006.

[4] Andrei Seryi, http://www.slac.stanford.edu/~seryi/, November 2005.

[5] V. Bargmann, L. Michel, and V.L. Telegdi. *Precession of the polarization of particles moving in a homogeneous electro-magnetic field*. *Phys. Rev. Lett.* 2(10):435-436, 1959.

[6] G. Mootgat-Pick, et al., *The role of polarized positrons and electrons in revealing fundamental interactions at the Linear Collider,* SLAC-PUB-11087, May 2005.

[7] Ken Moffeit and Mike Woods, *Laser System for a Compton Polarimeter*, IPBI TN-2003-2, December 2003, http://www.slac.stanford.edu/xorg/lcd/ipbi/notes/ComptonLaserSystem.pdf

[8] D. Cinabro, E. Torrence and M. Woods, ***Status of Linear Collider Beam Instrumentation Design,*** IPBI TN-2003-1, May 2003. Also available as an ALCPG Note LCD-ALCPG-03-0001 (2003).